JOURNAL OF AIRCRAFT
Vol. 46, No. 5, September–October 2009

Engineering Notes

Effect of Microtab on Reduction of Noise Due to Aircraft High-Lift Devices

Brian C. Kuo* and Nesrin Sarigul-Klijn†
University of California, Davis, Davis, California 95616

DOI: 10.2514/1.44125

I. Introduction

DEFINED as the "nonpropulsive noise of an aircraft in flight" in [1], noise produced by airframe components becomes significant during the approach-to-land phase of aircraft operations. Research efforts on identifying and understanding the noise sources associated with the individual airframe components, in particular, high-lift systems, have been undertaken by many researchers [2]. It has been confirmed experimentally in [3–5], and analytically by using empirical methods [6], that both leading-edge slats and trailing-edge flap side edges are the most important noise contributors from the high-lift systems to overall noise levels of an aircraft in approach.

The high-lift noise, intuitively thinking, is configuration dependent. Any increase in the deflection angle of slat and flap will lead to an increase in overall noise level. The larger the deflection angles are, the higher the noise level will be. This is due to the fact that the high-lift components are more loaded when their deflection angles are increased, generating what is referred to as the loading noise. Further, higher deflection angles may induce stronger vortex shedding and turbulent wake downstream which causes higher noise. Such intuitions were supported by experiments conducted at NASA Langley Research Center in 1998 and 2002 [7], which revealed that slat noise is generated due to its configuration setting angles. Khorrami et al. [8] hypothesized with 2-D unsteady computation that the vortex shedding at the slat trailing edge was responsible for the additional high-frequency spike observed only at higher slat angles. An acoustic whistling mechanism at the slat gap due to vortex shedding was later proposed by Tam and Pastouchenko [9] and Agarwal [10]. The theory supported that the simple vortex shedding and feedback mechanism resonating with gap tone frequency caused noise amplification and propagation. Similar observations were made for flap noise, as reported in [11,12]. Both references reported that the measured noise level at higher flap deflection angles exceeded the predicted noise level, which suggests that there might be an additional source contributor, most likely vortex instabilities, as a result of its interaction with the nearby flap upper surface. It may be noted that such phenomenon was not seen at lower settings of flap angles. These observations may infer that high-lift device noise level is directly affected by the configuration setting angles of slats and flaps. In general, high-lift device noise sources are present at wide frequency ranges of low-to-mid and mid-to-high. At a fixed observer location, under a constant flow speed, slat noise is dominant in the low-to-midfrequency range, and flap side-edge noise is dominant at the mid-to-high-frequency range as shown by both Guo and Joshi [13] and Guo et al. [14]. In this study, the proposed technique uses reduced deployment angles of both high-lift devices simultaneously to achieve the most effective noise reduction in different frequency domains. Aerodynamics performance also has to be carefully monitored to ensure no significant loss is present.

The objective of the current Note is to examine the effectiveness of a microtab device in airframe noise reduction. Reducing deployment setting angles of both slats and flaps, the associated noise can be alleviated. Loss in aerodynamic lift, as a result of the reduced high-lift settings, is compensated by use of a microtab device. The microtab device can be viewed as a small spanwise strip located at the pressure side of flap near the trailing edge, similar to a Gurney flap (Fig. 1). While deployed normal to local airfoil surface, the microtab device alters the local flowfield which leads to increased effective camber, and hence improves lift-to-drag ratio, similar to that of a Gurney flap introduced by Liebeck [15]. In the present work, a three-dimensional numerical analysis is presented and compared to sound pressure level (SPL) of the proposed microtab configuration at a specified far-field location to that of the baseline, that is, conventional configuration in approach, to see if any reduction in noise can be achieved.

II. Computational Study

The computational aeroacoustics simulations of a three-element high-lift wing derived from a Boeing 737 with and without microtab are studied. Detailed simulation procedures and models are presented as follows.

A. Acoustic Analogy

A Ffowcs Williams and Hawkings (FW-H) solver is embedded to the flow solver to calculate acoustic contents emitted to specified far-field observer locations. The time-accurate simulation was started with a nondimensional time step of 0.002 (scaled by freestream velocity and the stowed chord length) and was continued until

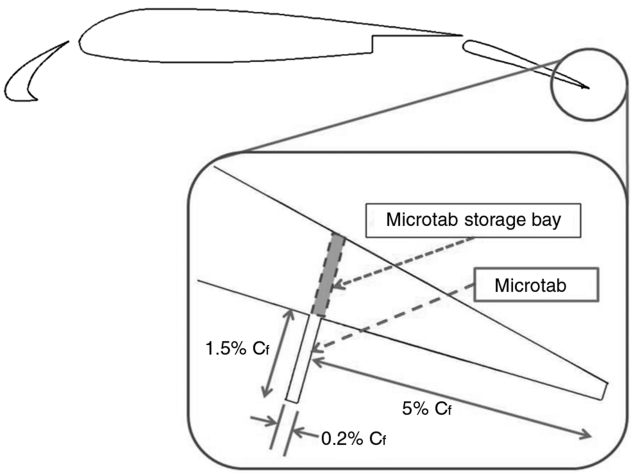

Fig. 1 Conceptual diagram of microtab device in the current study.

Presented as Paper 2864 at the 14th AIAA/CEAS Aeroacoustics Conference (29th AIAA Aeroacoustics Conference), Vancouver, British Columbia, Canada, 5–7 May 2008; received 3 March 2009; revision received 10 June 2009; accepted for publication 22 June 2009.

*Research Associate, Department of Mechanical and Aerospace Engineering Transportation Noise Control Center; bckuo@ucdavis.edu. Member AIAA.

†Professor, Department of Mechanical and Aerospace Engineering Transportation Noise Control Center; nsarigulklijn@ucdavis.edu. Associate Fellow AIAA.

Table 1 Geometrical setting of the high-lift models

	Baseline (HLD3030)	Proposed setting (HLD2020tab95)
Slat angle, deg	30	20
Flap angle, deg	30	20
Slat gap, $\%c$	2.95	2.95
Flap gap, $\%c$	1.27	1.27
Slat overhang, $\%c$	−2.5	−2.5
Flap overhang, $\%c$	0.25	0.25
Tab location, $\%c_f$	——	95
Tab height, h_t, $\%c_f$	——	1.5
Tab thickness, $\%c_f$	——	0.2
Angle of attack, deg	6	8.8

convergence on mean-flow and statistical quantities such as velocity magnitudes were achieved. Then a smaller nondimensional time step of 2.9×10^{-4} was used as the time step for acoustic predictions. A separate study on time-step selection showed that the initial time step of 0.002 was sufficient to obtain comparable results in aerodynamic properties, independent of temporal resolution. Initial transient effect due to changing time step was washed out before the acoustic solver was turned on. Another $10,000 \sim 12,500\mu$m time steps were then used as the unsteady pressure perturbation time history was collected and used as the input to the acoustic solver.

B. High-Lift Model and High-Fidelity Grid Topology

The high-lift airfoil profile used in this study was derived from a Boeing 737-type midspan airfoil from the University of Illinois, Urbana–Champaign's airfoil database. The unswept, untapered wing has an aspect ratio of 1.66. Detailed geometry settings for the two configurations simulated can be found in Table 1. A blunt trailing edge is assumed. The baseline had an angle of attack (AOA) of 6 deg, whereas AOA for the proposed setting case was chosen such that its mean lift was trimmed to the same level as that of the baseline to eliminate the effect of the aerodynamic loadings on the acoustic spectra.

Unstructured mesh was constructed to simulate the flow past the high-lift wing. Twenty to 25 points were used in the wall-normal direction to resolve the boundary-layer thickness properly. The first point away from the wall was placed at $1e$-$5c$, where c is the stowed wing chord length, such that y^+ is on the order of 1.5 or less. The computational boundary was placed at $50c$ in upstream and normal to the stream directions, $60c$ in the downstream direction, and $30b$ in the spanwise direction (b is the semispan length). The complete mesh sizes were between 2.5–2.75 million points.

C. Flow Solver and Flow Condition

The Reynolds-averaged Navier–Stokes (RANS) equations were solved by using a globally second-order upwind spatial discretization scheme, FLUENT 6.3. The time-accurate computations were performed by taking second-order time discretization and a dual-time-stepping technique. Thirty subiterations were used to ensure a minimum of four orders of magnitude drop in both the mean flow and turbulence model residuals during each time step that was obtained.

The one-equation Spalart–Allmaras (S–A) turbulence model [16] was chosen in this three-dimensional analysis, as it demonstrated better flow convergence capability and robust performance in a three-dimensional flowfield with high-lift geometry compared to the S-A model that the authors adopted in [17] for the two-dimensional analysis [17].

Validation of the CFD code has been done by the authors in a separate study, where noise coming from a 2-D auto cavity [18] was predicted and well captured compared to wind-tunnel measurement. In the current study, the freestream Mach number was prescribed at 0.17, which was appropriate with the incompressible flow assumption. The Reynolds number based on the stowed chord was about 13 million, and fully turbulent flow was assumed.

III. Results and Discussion

Acoustic spectra comparison in terms of SPL between the baseline and the proposed microtab configuration is shown in Fig. 2. To achieve noise reduction in a wide frequency range, the study configuration has both slats and flaps deflection angles reduced at the same time (see Table 1). Therefore, with the knowledge of "smaller deflection, lower noise" it can imply that slat noise reduction ought to be observed on the spectrum. An A-weighted SPL plot is also provided because the simulation Reynolds number is fairly close to the full-scale flight condition. The far-field observer location is placed at 270 deg directly below the wing root without any lateral shift.

Not much discrepancy is seen in the low-frequency domain, except that a significant rise in noise level is found for the microtab airfoil case at the low end of the frequency spectrum, less than 50 Hz. Converting the time history of both unsteady lift and drag into frequency spectra using Fourier transformation, it is confirmed that this low-frequency noise increase is due to stronger aerodynamic loading oscillation, particularly drag, when the microtab is deployed. This confirms the finding in the previous 2-D analysis [17]. Beyond 100 Hz and higher, the predicted noise level of the wing with microtab is 2–5 dB lower over the entire spectrum relative to the baseline configuration.

Figure 2b shows three notable noise spikes from the baseline at 315, 630, and 1260 Hz, respectively. The tone at 315 Hz can also be seen in the microtab case with approximately the same level of noise increase relative to the adjacent bands, as the other two tones are almost not present in the microtab case. In [17], the 2-D analysis revealed that the baseline configuration consisted of two noise spikes in the midfrequency range, which resulted from the slat cove region: one at 1500 Hz and the other at 4000 Hz, with the corresponding

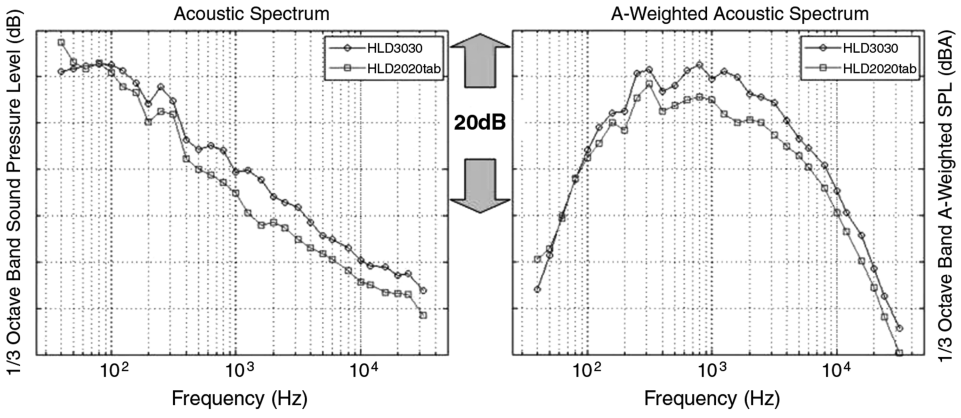

a) b)

Fig. 2 Comparison between the baseline configuration and the microtab setting.

Strouhal number St of 3.90 and 10.38, respectively. According to Dobrzynski and Pott-Pollenske [19] and Khorrami and Lockard [20], slat noise spectrum is composed of two components, one low-to-midfrequency broadband noise with $St = 1$–3, followed by another high-frequency tone that could reside anywhere between $St=$ 10–50. It can be inferred from the Strouhal number calculation using slat chord length and freestream velocity that the acoustic tone at 315 Hz was corresponding to the 1500 Hz tone in the 2-D study, with its Strouhal number slightly decreased to 2.78, whereas the tone at 1260 Hz corresponded to the 4 kHz tone, with its Strouhal number at 11.12. It is reasonable to attribute those two spikes to vortex shedding from slat cove cusp and slat trailing edge.

Meyer et al. [21] suggested an unsteady vortex shedding phenomenon due to Gurney flap deployment with the characteristic Strouhal number being in the range of 0.09–0.14. This observation helps explain the occurrence of the tone at 315 Hz for the airfoil with microtab case, given the fact that the high-lift settings have been reduced, but the peak level of the tone is surprisingly as large as that in the baseline configuration. Using the microtab height as a reference length and freestream velocity to calculate the microtab vortex shedding characteristic Strouhal number, it soon can be found that the tone at 315 Hz may comprise two components: one is slat cove vortex shedding from the cusp and the other is due to vortex shedding from the tab. In other words, the slat cove noise frequency coincides with the vortex shedding frequency from the tab in the spectrum.

The frequency spike at 630 Hz, based on the Strouhal number analysis, was not seen in [17], nor was it prominent in the tabbed airfoil case. Therefore, it is reasonable to indicate that tone comes from the flap side edge as a result of the three-dimensional effect. According to Dobrzynski et al. [4] and Choudhari et al. [7], the characteristic Strouhal number for flap side-edge noise could range from 5 to 12, as a result of vortex instability that causes interaction with the upper flap surface. Using flap chord length as a reference length, the Strouhal number for the 630 Hz tone can be calculated as 11.12. This tone, not seen in the tabbed airfoil case, further supports the view that the reduced high-lift configuration helps lower the noise generation and is in agreement with previous research efforts.

With the acoustic spikes identified based on Strouhal number analysis, the proposed high-lift configuration achieves an overall noise reduction of 2.3 dB by decreasing the deflection angles of both leading-edge slat and trailing-edge flap while the microtab device is deployed to compensate the lift loss. Such benefits obtained through numerical simulation will be confirmed using a different approach. A hot-wire measurement on the critical regions (e.g., flap side edge, slat trailing edge, and downstream of the tab) is desired before implementation to a practical aircraft.

The unsteady aerodynamics computations also showed a reduction in drag. With the addition of the $1.5\%c_f$ microtab in height in mind, the unsteady time-averaged drag was found to decrease by 5%. This is in accordance with the results from the previous 2-D analysis in [17] and Liebeck's observation reported in [15].

IV. Conclusions

Time-accurate RANS and FW-H acoustic analogy were used to study the three-dimensional unsteady flowfield and acoustic sources for a three-element high-lift wing with a microtab near the flap trailing edge. Reduced deflection of the high-lift devices is proposed to lower noise, with the microtab device compensating for the associated lift loss. This analysis indicates that the microtab configuration provides an overall airframe noise reduction of 2–5 dB over the entire frequency range. Noise reduction in the midfrequency range where human hearing is most sensitive is clearly evident. Deployment of the microtab shifted the acoustic energy toward the low-frequency domain and caused strong aerodynamic force oscillations, resulting in a tone spike at a very low frequency. However, looking at the A-weighted scale SPL spectrum, noise sources from the high-lift devices still dominated and it was the slat noise which seemed to determine the overall one-third octave band sound pressure level. Through the reduced high-lift settings with the microtab deployment, an overall 2.3 dB noise reduction was achieved. To validate the computational results, in particular, the Strouhal number analysis on the narrowband tones, a hot-wire measurement is planned as the next stage of the research direction.

References

[1] Crighton, D. G., "Airframe Noise in Aeronautics of Flight Vehicles: Theory and Practice," *Noise Sources*, Vol. 1, NASA RP 1258, pp. 391–447, 1991.

[2] Macaraeg, M. G., "Fundamental Investigation of Airframe Noise," AIAA Paper 1998-2224, 1998.

[3] Hayes, J., Hornes, W. C., Soderman, P. T., and Bent, P. H., "Airframe Noise Characteristics of a 4.7% Scale DC-10 Model," AIAA Paper 1997-1594, 1997.

[4] Dobrzynski, W., Nagakura, K., Gehlhar, B., and Buschbaum, A., "Airframe Noise Studies on Wing with Deployed High-Lift Devices," AIAA Paper 1998-2337, 1998.

[5] Davy, R., and Remy, H., "Airframe Noise Characteristics on a 1/11 Scale Airbus Model," AIAA Paper 1998-2355, 1998.

[6] Guo, Y. P., Yamamoto, K., and Stoker, R., "Component-Based Empirical Model for High-Lift System Noise Prediction," *Journal of Aircraft*, Vol. 40, No. 5, Sept.–Oct. 2003, pp. 914–922. doi:10.2514/2.6867

[7] Choudhari, M., Lockard, D., Macaraeg, M., Singer, B., Streett, C., Neubert, G., Stoker, R., Underbrink, J., Berkman, M., Khorrami, M., and Sadowski, S., "Aeroacoustic Experiments in the Langley Low-Turbulence Pressure Tunnel," NASA TM 2002-211432, Feb. 2002.

[8] Khorrami, M., Berkman, M., and Choudhari, M., "Unsteady Flow Computations of a Slat with a Blunt Trailing Edge," *AIAA Journal*, Vol. 38, No. 11, Nov. 2000, pp. 2050–2058. doi:10.2514/2.892

[9] Tam, C., and Pastouchenko, N., "Gap Tones," *AIAA Journal*, Vol. 39, No. 8, Aug. 2001, pp. 1442–1448. doi:10.2514/2.1494

[10] Agarwal, A., "The Prediction of Tonal and Broadband Slat Noise," Ph.D. Thesis, Pennsylvania State Univ., State College, PA, May 2004.

[11] Brooks, T., and Humphreys, N., "Flap Edge Aeroacoustics Measurements and Predictions," AIAA Paper 2000-1975, 2000.

[12] Streett, C., Lockard, D., Singer, B., Khorrami, M., and Choudhari, M., "In Search of the Physics: The Interplay of Experiment and Computation in Airframe Noise Research: Flap-Edge Noise," AIAA Paper 2003-0979, 2003.

[13] Guo, Y. P., and Joshi, M., "Noise Characteristics of Aircraft High Lift System," *AIAA Journal*, Vol. 41, No. 7, July 2003, pp. 1247–1256. doi:10.2514/2.2093

[14] Guo, Y. P., Joshi, M., and Yamamoto, K., "Surface Pressure Fluctuation on Aircraft Flaps and Their Correction with Farfield Noise," *Journal of Fluid Mechanics*, Vol. 415, July 2000, pp. 175–202. doi:10.1017/S0022112000008740

[15] Liebeck, R., "Design of Subsonic Airfoil for High Lift," *Journal of Aircraft*, Vol. 15, No. 9, Sept. 1978, pp. 547–561. doi:10.2514/3.58406

[16] Spalart, P. R., and Allmaras, S. R., "A One-Equation Turbulence Model for Aerodynamic Flows," AIAA Paper 1992-0439, 1992.

[17] Kuo, B. C., and Sarigul-Klijn, N., "Numerical Investigation of Micro-Tab in Airframe Noise Reduction," AIAA Paper 2007-3452, 2007.

[18] Dahl, M., "Third Computational Aeroacoustics (CAA) Workshop on Benchmark Problems: Category 6 Automobile Noise Involving Feedback," NASA CP-2000-209790, 2000.

[19] Dobrzynski, W., and Pott-Pollenske, M., "Slat Noise Source Studies for Far-Field Noise Prediction," AIAA Paper 2001-2158, 2001.

[20] Khorrami, M., and Lockard, D., "Effects of Geometric Details on Slat Noise Generation and Propagation," AIAA Paper 2006-2664, 2006.

[21] Meyer, R., Hage, W., Bechert, D. W., Schatz, M., and Thiele, F., "Drag Reduction on Gurney Flaps by Three-Dimensional Modifications," *Journal of Aircraft*, Vol. 43, No. 1, Jan.–Feb. 2006, pp. 132–140. doi:10.2514/1.14294